Biogeosciences Discuss., doi:10.5194/bg-2016-12, 2016
Manuscript under review for journal Biogeosciences
Published: 23 February 2016

Biogeosciences Discussions
Open Access
EGU

No tropospheric ozone impact on the carbon uptake by a Belgian pine forest

Lore Verryckt[1], Maarten Op de Beeck[1], Johan Neirynck[2], Bert Gielen[1], Marilyn Roland[1], and Ivan A. Janssens[1]

[1]Department of Biology, University of Antwerp, Wilrijk, 2610, Belgium

[2]Research Institute for Nature and Forest, Geraardsbergen, 9500, Belgium

Correspondence to: L. Verryckt (lore.verryckt@uantwerpen.be)

Abstract High stomatal ozone (O_3) uptake has been shown to negatively affect crop yields and the growth of tree seedlings. However, little is known about the effect of O_3 on the carbon uptake by mature forest trees. This study investigated the effect of high O_3 events on gross primary production (GPP) for a Scots pine stand near Antwerp, Belgium over the period 1998-2013. Stomatal O_3 fluxes were modelled using in situ O_3 concentration measurements and a multiplicative stomatal model, which was parameterised and validated for this Scots pine stand. Ozone-induced GPP reduction is most likely to occur during or shortly after days with high stomatal O_3 uptake. Therefore, a GPP model parameterised for days with low stomatal O_3 uptake rates was used to simulate GPP during periods of high stomatal O_3 uptake. Eventual negative effects of high stomatal O_3 uptake on GPP would then result in an overestimation of GPP by the model during or after high stomatal O_3 uptake events. The O_3 effects on GPP were linked to AOT40 and POD_y. Although the critical levels for both indices were exceeded in every single year, no significant negative effects were found of ozone on GPP and no correlations between GPP residuals and AOT40 and POD_y were found. Overall, we conclude that no O_3 effects were detected on the carbon uptake by this Scots pine stand.

1 Introduction

Tropospheric ozone (O_3) is a secondary air pollutant that has the potential to negatively affect vegetation, leading to reduced growth and carbon sequestration potential (ICP Vegetation, 2012; Middleton, 1956). Background concentrations of tropospheric O_3 have increased with 36 % since pre-industrial times (IPCC, 2001) and are projected to further increase considerably until about 2050 (IPCC, 2007). Depending on the scenarios, background O_3 levels might either increase or decrease after 2050 (IPCC, 2007).

In recent years, many studies have been conducted to investigate the mechanisms underlying the O_3 impacts on vegetation. Ozone reduces plant growth by altering photosynthetic rates, carbohydrate production, carbon sequestration, carbon allocation, and carbon translocation (Reich and Amundson, 1985;Andersen et al., 1997;Beedlow et al., 2004). Once O_3 enters the leaves through the stomata, it can affect plant growth by direct cellular damage (Mauzerall and Wang, 2001), leading to visible leaf injury and reduced leaf longevity (Noble and Jensen, 1980). In response to O_3, respiratory processes increase, which will also effect the tree's carbon balance (Darall, 1989). Skärby et al. (1987) proved that dark respiration of Scots pine shoots increased after long-term exposure to a low level of O_3. Protective responses, such as compensation (e. g. repair of injured tissue), avoidance

Biogeosciences Discuss., doi:10.5194/bg-2016-12, 2016
Manuscript under review for journal Biogeosciences
Published: 23 February 2016

(e. g. stomatal closure), and tolerance (e. g. alteration of metabolic pathways), all consume carbon and, hence, resistance to O_3 damage costs energy. The size of this cost affects the amount of carbon remaining to support growth (Skärby et al., 1998).

To assess the impact of O_3, several indices have been created, e. g. AOT40 (ppb h), the cumulated O_3 concentration in excess of a threshold of 40 ppb, and POD_y, the accumulated O_3 flux above a flux threshold y (nmol m^{-2} s^{-1}). Critical levels, quantitative estimates of exposure to O_3 above which direct adverse effects may occur (CLRTAP, 2015), have been determined for these indices based on O_3 dose-response relationships from fumigation experiments with enhanced O_3 concentrations (Karlsson et al., 2004). The magnitude of the O_3 impact on plants depends on the intensity of O_3 exposure, environmental factors influencing both plant photosynthesis and the O_3 flux to plant surfaces, and plant species-specific defensive mechanisms (Musselman and Massman, 1999). Because of the variable plant responses to similar O_3 concentrations, the question arises whether widely applicable tolerable limits of O_3 concentration exist (Skärby et al., 1998).

While high stomatal O_3 fluxes have been shown to affect crop yields and tree seedlings, it is not sure whether O_3 uptake or O_3 flux also negatively affects the carbon uptake by mature forest trees. Many studies determined the effect of O_3 on seedlings and young trees (Buker et al., 2015), but little is known about the effect on mature trees. When scaling up the results from seedlings to mature trees the resulting data should be viewed with caution, due to differences in energy budgets, canopy:root balances and architecture and carbon allocation patterns (McLaughlin et al., 2007;Chappelka and Samuelson, 1998). In addition to the uncertainties related with the up-scaling from seedlings to mature trees, data from controlled experiments should also be used with caution, because trees can react differently in field conditions (Skärby et al., 1998). The effect of O_3 uptake on carbon uptake under ambient O_3 concentrations by trees has hardly been studied in situ. Some studies showed reductions in plant growth due to stomatal O_3 uptake (Zapletal et al., 2011;Fares et al., 2013;Yue and Unger, 2013), while other studies did not show any effect (Zona et al., 2014;Samuelson, 1994). Whether or not an effect of stomatal O_3 uptake was found was species- and site- specific, and there is a clear need for more studies investigating the effect of O_3 on carbon uptake by mature trees in the field (Chappelka and Samuelson, 1998).

Here we investigate the effect of high O_3 events on gross primary production (GPP) for a Scots pine stand in Flanders, Belgium. At current ambient O_3 levels, critical levels for both AOT40 and POD_1 are already being exceeded in this Scots pine stand (Neirynck et al., 2012). This indicates that even at current ambient O_3 levels tree productivity might be affected. Ozone-induced GPP reduction is most likely to occur during or shortly after days with high stomatal O_3 uptake. An effect of stomatal O_3 uptake on GPP can be detected when a GPP model parameterised for days with low stomatal O_3 uptake rates is extrapolated to high stomatal O_3 uptake events – i. e., days where an effect on GPP is assumed - and the model overestimates GPP during these events. This study therefore tests the hypothesis that GPP of the studied pine forest is reduced during or shortly after high stomatal O_3 uptake events.

2 Materials and methods

Biogeosciences Discuss., doi:10.5194/bg-2016-12, 2016
Manuscript under review for journal Biogeosciences
Published: 23 February 2016

2.1 Study area

The study area consisted of a 2-ha Scots pine stand in a 150-ha coniferous/deciduous forest named 'De Inslag', situated in Brasschaat (+51° 18' 33'' N, +04° 31' 14'' E), northeast of the Antwerp agglomeration and east-northeast of the Antwerp harbour (Neirynck et al., 2008). The site has a temperate maritime climate with a mean annual temperature of 11 °C and a mean annual precipitation of 830 mm (Neirynck et al., 2008).

The soil has been classified as Albic Hypoluvic Arenosol (Gielen et al., 2011), a moderately wet sandy soil with a distinct humus and/or iron B-horizon (Janssens et al., 1999). The sandy layer overlays a clay layer which is situated at a depth of 0.7 - 2 m. As a result of the poor drainage groundwater depth is typically high, fluctuating between 0.5 and 2 m (Carrara et al., 2003).

The trees were planted in 1929 (Neirynck et al., 2008). In 1995, tree density amounted to 542 trees ha^{-1}. In the autumn of 1999, the forest was thinned, which resulted in 376 trees ha^{-1} in 2001. With a peak in leaf area index (LAI) of 1.3 ± 0.5 m^2 m^{-2} in 2007 (Op de Beeck et al., 2010) and an average LAI of 1.2 ± 0.5 m^2 m^{-2} in the period 1998-2007, the stand canopy is very sparse. Only two needle-age classes are present: current-year needles and one-year-old needles (Op de Beeck et al., 2010).

2.2 Measurements: meteorology, O_3, GPP, and LAI

In this study, continuous measurements over the period 1998 - 2013 were used, excluding 1999 and 2003 due to poor data quality or coverage. Different meteorological variables were measured on a tower with a height of 41 m, set up in 1996 (Gielen et al., 2013). A sonic anemometer (Model Solent 1012R2, Gill Instruments, Lymington, UK) measures the wind velocity (WV; m s^{-1}). Meteorological data include vertical profiles of air temperature (T_{air}; °C) and humidity (RH; (%) (HMP 230 dew point transmitter and PT100, Vaisala, Finland) in aspirated radiation shields at 2, 24 and 40 m height. Wind speed measurements (LISA cup anemometer, Siggelkow GMBH, Germany) are conducted at 24, 32 and 40 m height. At the top of the tower, ingoing and outgoing short-wave and long-wave radiation are measured by a CNR1-radiometer (pyranometer/pyrgeometer, Kipp and Zonen, the Netherlands) and a CMP6-pyranometer (Kipp and Zonen, the Netherlands). A wind vane (potentiometer W200P, Campbell, UK) is mounted on a tower rail. Rainfall is registered by a tipping bucket rain gauge (NINA precipitation pulse transmitter, Siggelkow GMBH, Germany). Both T_{air} and RH are used to calculate vapour pressure deficit (VPD; kPa). Soil temperature (T_{soil}; °C) is measured at 9 cm below the soil surface with temperature probes (Didcot DPS-404, UK). Soil water content (SWC; m^3 m^{-3}) was measured at 25 cm below the soil surface using a TDR (Time Domain Reflectometer) sensor at three days to biweekly resolution and subsequently interpolated to obtain daily estimates, taking into account water inputs via precipitation (Gielen et al., 2010). Soil water potential (SWP; MPa) was derived from SWC measurements (m^3 m^{-3}) with the model of van Genuchten (van Genuchten, 1980). All climatic variables were measured every 10 seconds and half hourly means were stored on a data logger (Campbell CR1000, UK) in an air-conditioned cabinet adjacent to the tower. Data gaps were filled with data from nearby weather stations.

Vertical profiles of O_3 concentrations are being measured at two inlets above the canopy (at 24 and 40 m) using an UV Photometric Analyzer (model TEI 49I, Thermo Environmental Instruments). CO_2 concentrations (ppm) are

Biogeosciences Discuss., doi:10.5194/bg-2016-12, 2016
Manuscript under review for journal Biogeosciences
Published: 23 February 2016

measured using an infrared gas analyser (IRGA) (Model LI-6262, LI-COR Inc., Lincoln, NE, USA). The vertical CO_2 flux between the forest and the atmosphere, net ecosystem exchange (NEE), was measured with the eddy covariance technique following standard data quality procedures (Carrara et al., 2003;Gielen et al., 2013;Carrara et al., 2004). Gross primary production (µmol C m^{-2} s^{-1}) is derived from NEE data, by subtracting the modelled total (autotrophic and heterotrophic) ecosystem respiration from the measured NEE. The ecosystem respiration or total carbon loss is modelled with standardised algorithms as presented in Falge et al. (2001).

The LAI time series for the Brasschaat forest was reconstructed based on the historical data. The general approach was to use the fragmentary LAImax data that were measured by Gond et al (1999) in 1997, by Konôpka et al. (2005) in 2003 and by Op de Beeck et al. (2010) in 2007. The latter was done with hemispherical pictures while the first in 1997 and 2003 were done with the LAI-2050 instrument (LI-COR, Lincoln, Nebraska, USA). To assure consistency across the time series, measurements were corrected for clumping by using the factor 0.83 (Jonckheere et al., 2005). All LAImax measurements were interpolated lineairly to derive LAImax values for the missing years. The thinning event in 1999 was accounted for by subtracting the removed leaf biomass by using the allometric relations from Yuste et al. (2005) and specific leaf are measurements from Op de Beeck et al. (2010). The seasonal pattern of the Op de Beeck et al. (2010) measurements was used and kept constant over the entire time series.

2.3 Stomatal conductance measurements

During the summers of 2007 and 2013, stomatal conductance to H_2O ($g_{st,\,H2O}$) of Scots pine needles was measured at the site. These $g_{st,H2O}$ measurements were based on gas exchange measurements (photosynthesis and transpiration), which were carried out with a leaf cuvette connected to an IRGA (LI-6400, LI-COR, Lincoln, Nebraska, USA).

Stomatal measurements were carried out in highly different environmental conditions during 2007 (cold and wet summer) and 2013 (warm and dry summer). Diurnal stomatal measurements and stomatal responses to PAR, T_{air}, and VPD, both on one-year-old needles and on current-year needles, were carried out during the summers of 2007 (Op de Beeck et al., 2010) and 2013. All measurements in 2007 were carried out on the needles of the two trees closest to the tower, both in the lower and the upper canopy. In 2013 only the tree closest to the tower was accessible for measurements. The total number of sets of needles on which measurements were carried out, amounts to 10 in 2007 and 16 in 2013. The LI-6400 instrument calculated the $g_{st,H2O}$ assuming the whole area of the cuvette (2x3 cm) was covered with the needles. To obtain the g_{st} to O_3 (from here on referred to as 'g_{st}') of the six or eight needles in the cuvette, two corrections needed to be made: one for the needle area, because needles did not completely cover the area of the cuvette, and a second one for converting the data from $g_{st,\,H2O}$ to g_{st}.

The width of the needles was measured at 40 x magnification under a binocular microscope (M3 Wild, Wild Heerbrugg, Gais, Switzerland) in combination with an ocular equipped with a reticule (Leitz, Wetzlar, Germany, periplan, GW 10xm). The width per needle was measured at three places: at the top, in the middle, and at the base. An average of those three measurements was multiplied by the length of the needle inside the cuvette, 3 cm. After measuring the needle area with a microscope, the $g_{st,H2O}$ data were corrected for the lower needle area. These data

Biogeosciences Discuss., doi:10.5194/bg-2016-12, 2016
Manuscript under review for journal Biogeosciences
Published: 23 February 2016

were multiplied by 0.61, which is the ratio of the molecular diffusivities of water vapour and O_3 in the air, to convert from $g_{st,H2O}$ to g_{st}.

2.4 Multiplicative stomatal model: description

Stomatal conductance was modelled using the multiplicative g_{st} model, first described by Jarvis (1976). The model has been developed to calculate species-specific g_{st} according to phenology and environmental conditions (Emberson et al., 2000) and is described in detail in Appendix A.

We modified the model to make it more applicable for Scots pine. In this modified model (Eq. 1) PAR, T_{air}, VPD, and SWP influence the range between g_{max} and g_{min} instead of g_{max} and zero. This modification was needed, because in the Brasschaat pine forest stomata never completely close, hence g_{st} is never zero (Op de Beeck et al., 2010).

$$g_{st} = g_{max} * f_{phen} * (f_{min} + (1 - f_{min}) * (f_{PAR} * f_T * f_{VPD} * f_{SWP}) \quad (1)$$

Here g_{st} is the stomatal conductance to O_3 and g_{max} is the maximal stomatal conductance to O_3. The functions f_{PHEN}, f_{PAR}, f_T, f_{VPD}, and f_{SWP} represent the modification of g_{max} by, respectively, phenology, PAR, T_{air}, VPD, and SWP. The function f_{min} is the ratio of g_{min} and g_{max} where g_{min} is the minimal stomatal conductance to O_3 (see Appendix A for more detailed information). Impaired stomatal aperture mechanisms (stomatal sluggishness) due to ozone exposure (Paoletti and Grulke, 2010) were not included in the model development.

2.4.1 Multiplicative stomatal model: parameterisation and validation

For the optimisation of the parameters of the different functions in the model, we assumed that the phenology function was 1. This was deemed a fair assumption, because $g_{st,H2O}$ was measured on mature needles in the summer (July/August 2007 and 2013), in the middle of the growing season.

The data set, including measured g_{st}, PAR, T_{air}, VPD, and SWP, was split into two subsets by grouping odd and even rows for data sorted by PAR. One set was then used for parameterisation, the other for validation. The stomatal model was parameterised using the computer program Matlab (version 2013a). The optimisation of all parameters was done with the function 'lsqcurvefit' in Matlab. It finds the best parameter values, starting with an initial value, to best fit the function of the stomatal model to measured g_{st} and can thus be used to fit a nonlinear function with more than two independent variables. All parameters of f_{PAR}, f_{Tair}, f_{VPD}, and f_{SWP} were optimised separately, with initial values that were estimated visually from plots of the functions to the dataset.

2.4.2 Multiplicative stomatal model: model evaluation

The parameterised multiplicative stomatal model was then tested against the validation dataset. Measured g_{st} values were plotted against the modelled g_{st} values. A linear function $y = ax + b$ was fitted, where 'a' should be not significantly different from one ($p > 0.05$) and 'b' should be not significantly different from zero ($p > 0.05$) for both parameterisation and validation dataset. We evaluated the model performance with the following statistics: the coefficient of determination or R squared (R^2) as a goodness-of-fit measure and error-based measures including

Biogeosciences Discuss., doi:10.5194/bg-2016-12, 2016
Manuscript under review for journal Biogeosciences
Published: 23 February 2016

mean bias (MB), relative mean error (RME), Willmott's index of agreement (d), model efficiency (ME), root mean squared error (RMSE), and its systematic ($RMSE_s$) and unsystematic component ($RMSE_u$). In Appendix B these error-based statistics are explained.

The measured g_{st} was plotted in function of the different input variables (PAR, T_{air}, VPD, and SWP) and the boundary function of each plot was fitted. This was done in order to test how well the obtained parameter values were estimated in function of the measured g_{st}.

2.5 Canopy model

We applied a canopy model to scale up g_{st}, measured at leaf level, to the canopy level. The canopy model consists of different horizontal leaf layers and includes a radiation transfer model (Goudriaan, 1977), a solar elevation model (Campbell and Norman, 1998) and the modified multiplicative stomatal model (Emberson et al., 2000). The model is described in detail in Appendix C.

The model calculates half-hourly totals of the total, stomatal, and non-stomatal O_3 fluxes based on the following input variables: day of year, hour, Rg, T_{air}, VPD, SWP, O_3 concentration above the canopy (24m), LAI, and friction velocity u*. The total O_3 flux (nmol m^{-2} s^{-1}) for the whole canopy was the product of O_3 concentrations (ppb) and g_{tot} (mol (m^2 ground $area^{-1}$) s^{-1}) (Musselman and Massman, 1999). This last parameter was calculated with an electrical model (Eq. 2).

$$g_{tot} = \left(\frac{1}{g_{aero}} + \frac{1}{g_{bl}} + \frac{1}{g_{can}}\right)^{-1} \quad (2)$$

where g_{tot} is the total conductance to O_3 (mol (m^2 ground $area^{-1}$) s^{-1}); g_{aero} is the aerodynamic conductance and is set to 1; g_{bl} is the boundary layer conductance to O_3; g_{can} is the canopy conductance.

The boundary layer conductance to O_3 was calculated with the following formula (Baldocchi et al., 1987):

$$g_{bl} = \frac{K * u^*}{2 * \frac{Sc^{\frac{2}{3}}}{Pr}} * 44.64 \quad (3)$$

where K is the von Karman constant (0.43); u* (m s^{-1}) is the friction velocity, which is derived from the measured momentum fluxes; Sc is the Schmidt number (1.07 for O_3); Pr is the Prandtl number (0.72 for O_3); 44.64 mol m^{-3} is the molar density of air, and is applied for converting the unit of g_{bl} from m s^{-1} to mol m^{-2} s^{-1}.

The canopy conductance consisted of a stomatal and a non-stomatal component. Since the stomatal component varies throughout the canopy, the canopy was divided into eight sublayers so that the leaves were evenly distributed between the horizontal layers. Dividing the canopy into sufficient sublayers was necessary in order to model fluxes well. Eight sublayers were considered to be sufficient, as indicated in a sensitivity test with more and less sublayers. For each leaf layer, the model calculates g_{st} for sunlit and shaded needles, taking the solar elevation angle into account. Non-stomatal conductance was assumed to be constant over the canopy and was set at 0.16. This value was derived from long-term O_3 flux measurements in Brasschaat (Neirynck et al., 2012).

Biogeosciences Discuss., doi:10.5194/bg-2016-12, 2016
Manuscript under review for journal Biogeosciences
Published: 23 February 2016

The stomatal and non-stomatal O_3 fluxes (nmol m^{-2} s^{-1}) were calculated by multiplying the proportion of g_{st} and g_{ns} of the canopy per ground area with the O_3 concentration.

These obtained half-hourly fluxes were aggregated to daily fluxes. These daily fluxes were averaged in order to know the average daily O_3 uptake by the canopy for the different years. The ratio F_{st}/F_{tot} was calculated and this gives an indication of the contribution of the stomatal O_3 flux to the total O_3 flux.

2.6 Ozone effects

A feed-forward back propagation Artificial Neural Network (ANN) in Matlab (Matlab Matworks R2013a, The MathWorks Inc., Natick, Massachusetts, USA) was used to simulate GPP of the Scots pine forest. The ANN, which contained 10 nodes organised in 1 layer, was trained with 70% data random selected data measured data and validated based on the remaining 30% of data set (R^2=0.72). The daily GPP data of the growing seasons between 1998-2013, except 1999 and 2003, were used as dependent target variable, whereas year, day of year, T_{min}, T_{max}, T_{mean}, average VPD, SWC, Rg, average T_{soil}, and average WV of these periods were used as independent input variables. Daily totals of the variables were used, with the exception of VPD, T_{soil}, and WV for which daily averaged values were used.

To obtain an O_3-damage free GPP model, data from days for which an O_3 effect was expected were removed from the dataset. These were the days with stomatal O_3 uptake values in the upper 2%, 5 %, and 10% of stomatal O_3 flux. As the results of a 2% and 10% cut-off were equal to a 5% cut-off, we report only results of a 5% cut-off. With 2/3 of the data from days with low stomatal O_3 uptake, the artificial neural network was trained. The other 1/3 was used to test the model. This O_3-damage free GPP model was then run with all data. The absolute and relative differences in GPP accumulated over the growing season between EC-derived and modelled values were calculated, to investigate whether or not there was a reduction of GPP.

The relation between the residuals of total GPP and both AOT40, POD_1 and POD_2 was examined. Therefore, a linear fit between the residuals and the indices was made. A significant negative correlation would exist if the slope is significant different from 0 ($p < 0.05$) and intercept is not significant different from 0 ($p > 0.05$). These yearly GPP residuals were also plotted to the stomatal O_3 flux to investigate their relation and a linear fit was made of which the significance was tested. If GPP was increasingly overestimated in the presence of higher stomatal O_3 fluxes, this would indicate a deleterious O_3 effect.

Ozone effects possibly appear and last during a period of several days after the O_3 peaks, and as a result they will not be detected in the above analyses. Due to these possibly lag effects of O_3, the above analyses were repeated, but now excluding the days with high stomatal O_3 uptake along with the two subsequent days removed from the training and testing datasets.

Biogeosciences Discuss., doi:10.5194/bg-2016-12, 2016
Manuscript under review for journal Biogeosciences
Published: 23 February 2016

3 Results

3.1 Measurements: meteorology, GPP, and LAI

A fingerprint of the multi-annual average diel and seasonal pattern in the measured data is shown in Fig. 1. This figure gives a good overview of how meteorology and GPP typically changed over time in this forest; interannual anomalies from the average patterns can be found in Fig. S1. Distinct daily and seasonal patterns can be observed for T_{air}, R_g, and VPD, reaching highest values in summer, in the afternoon. Similar patterns can also be observed in GPP, which basically follows the pattern of Rg. As seen on Fig. 1, the photosynthetic period extends, on average, from day of year 115 (end of April) till day of year 300 (end of October). The precipitation and SWP time series are provided in Fig. 2, while changes in LAI over time are shown in Fig. 3The yearly maximum LAI ranged from 1.4 to 1.9 m^2 m^{-2}. The thinning of the forest in 1999 can clearly be observed in the LAI pattern. After the thinning, the canopy never fully closed.

3.2 Multiplicative stomatal model and simulated O_3 fluxes

The best fitting parameter values for the multiplicative stomatal model are presented in Table 1 and different statistics to evaluate the model performance are presented in Table 2. For the parameterisation dataset, the measured data were fitted against modelled g_{st} and plotted in Fig. 4. The slope of the linear fit was not significantly different from 1 ($p > 0.05$) and the intercept was not significantly different from 0 ($p > 0.05$). Model evaluation for the validation dataset was equally good as for the parameterisation dataset (Table 2). Also in the linear fit for the validation set (Fig. 4, B), the slope was not significantly different from 1 ($p > 0.05$) and the intercept was not significantly different from 0 ($p > 0.05$).

In Fig. 5 the measured g_{st} was plotted against the different model input variables: PAR, T_{air}, VPD, and SWP, and for each plot the boundary function was fitted.

The average daily O_3 fluxes for the different years are presented in Fig. S2. The daily total F_{st} ranges from 1.42 to 2.00 nmol O_3 m^{-2} day^{-1}. In 2011 the daily total F_{st} was the lowest, while in 2002 the highest stomatal flux was reached. The annual average ratio F_{st}/F_{tot} varied between 24-28 % (Fig. S2). We observed the lowest ratios in the beginning and at the end of the growing season. Above-average ratios were observed at the peak of the growing season.

3.3 Ozone effects on GPP

Total GPP (mol C m^{-2} day^{-1}) was calculated for days with low stomatal O_3 uptake, high stomatal O_3 uptake and for the entire growing season, using both the EC-derived GPP data and the modelled GPP data (Table 3). For days with low stomatal O_3 uptake, the average daily total GPP was 0.48 mol C m^{-2} day^{-1}, and the models reproduced GPP very well (Table 3). When we calculated total GPP for days with high stomatal O_3 uptake, the EC-derived fluxes were much higher than for the days with low stomatal O_3 uptake. This was probably due to the higher irradiation that typically occurs during high O_3 events and stimulates GPP. The higher GPP, however, also suggests that negative O_3 effects on GPP were highly unlikely. This is exacerbated by the fact that our models almost

Biogeosciences Discuss., doi:10.5194/bg-2016-12, 2016
Manuscript under review for journal Biogeosciences
Published: 23 February 2016

consistently underestimate GPP during high O_3 events (Table 3), whereas we hypothesised the exact opposite, namely that the models would overestimate GPP during these events because they were parameterised for low O_3 days. We also observed no differences between both models, suggesting no lagged O_3 effects on GPP (Table 3).

A weak, negative correlation between total GPP residuals and F_{st} exists for the GPP model trained without days with high stomatal O_3 uptake (Fig. 7, A), while a small positive correlation is shown for the GPP model which tested for lag effects of O_3 (Fig. 7, B). However, these differences were not statistically significant at $p<0.05$. For both models, correlations between total GPP residuals and AOT40, and between total GPP residuals and both POD_1 and POD_2 existed. These correlations were also not statistically significant at $p<0.05$ (Fig. 7, C, D, E, F, G, and H).

4 Discussion

4.1 Multiplicative stomatal model

All statistics shown in Table 2 clearly indicated that the fitted multiplicative stomatal model performed well. For both parameterisation and validation datasets, the model explained 72 % of the variance in g_{st}. For both datasets, slope and intercept of the linear regression lines of measured versus modelled g_{st} were not significantly different from 1 and 0, respectively (Fig. 4). Moreover, the model efficiency (ME in Table 2) of 0.72 and the Wilmott's index (d) close to 1 both indicate that the modelled values matched the measured values well. A good model provides low root-mean-square error (RMSE), while the systematic component ($RMSE_s$) should approach zero and the unsystematic component ($RMSE_u$) should approach RMSE (Willmott et al., 1985), which was the case for this model. Low mean bias (MB) and low mean relative error (MRE) further indicated very good performance. The good performance of the model can also be observed in Fig. 5, in which the boundary lines represented the response of g_{st} to the independent variables when other variables were not limiting (Martin et al., 1997). The boundary lines fitted close to the data points, which is an indication of a good model, because the multiplicative stomatal model is based on the assumption that the variables act more or less multiplicatively and independently from each other (Grüters et al., 1995).

Multiplicative stomatal models based on Jarvis (1976) have been parameterised earlier for generic Scots pine forests in Europe (Mills et al., 2011;Buker et al., 2015) and used to estimate critical levels for this species. However, the empirical the dose-response relationship for Scots pine is based on only one two-year fumigation study on small seedlings and, therefore, high uncertainty exists in the modelled O_3 impact on Scots pine growth.

The parameterisation of Mills et al. (2011) and Büker et al. (2015) differ from that of this study in a number of parameters. First, the needles of the Scots pine stand in Brasschaat had a higher night-time g_{st} (g_{min}) and will therefore take up more O_3 at night. Maximal g_{st}, in contrast, is lower in Brasschaat than estimated for other Scots pine forests, implying that during episodes of high O_3 concentrations, the Brasschaat site is unlikely to take up very high amounts of O_3. This may have contributed to the absence of a clear O_3 response at our study site. Also the Scots pine stand in Brasschaat is less sensitive to drought stress than the generic model, due to a higher VPD_{max} and a wider SWP range. The wider SWP range is mainly due to a clearly lower SWP_{max}. These differences between the parameter values and, hence, in g_{st} for generic Scots pine forests and for the Scots pine stand in Brasschaat will

Biogeosciences Discuss., doi:10.5194/bg-2016-12, 2016
Manuscript under review for journal Biogeosciences
Published: 23 February 2016

lead to different critical levels and under- or overestimation of possible O_3 damage. Species-specific parameterisation is important, but site-specific parameterisation is clearly important as well.

4.2 Stomatal O_3 fluxes at canopy scale

The stomatal O_3 flux contributed on average for 26 % to the total O_3 flux over the study period (Fig. S2). This fraction is similar to the 21 % stomatal O_3 flux in a Danish Norway spruce stand (Mikkelsen et al., 2004) and the 30 % stomatal O_3 flux in *Quercus ilex* in Italy (Vitale et al., 2005;Gerosa et al., 2005). Cieslik (2004) showed that in Southern Europe stomatal O_3 flux of different vegetation types, such as pine forest and Mediterranean shrubs, is typically less than 50 % of the total O_3 flux. A five-year study on a Mediterranean *Pinus ponderosa* stand showed a stomatal O_3 flux contribution of 57 % (Fares et al., 2010). Clearly species- and site-specific differences such as tree age or micro-climate are introducing large variability in stomatal O_3 uptake (Neirynck et al., 2012).

The low relative stomatal O_3 flux in the Scots pine stand in Brasschaat could be the result of the sparse canopy with low LAI. Although no relation between stomatal O_3 flux and LAI was found in a previous site study on this site (Neirynck et al., 2012), interannual and seasonal variation in LAI is very small, rendering such a correlation analysis very difficult.

4.3 Ozone effects on GPP

Although our models reproduced GPP very well, we did not observe immediate or lagged effects of high stomatal O_3 uptake on GPP (Table 3; Fig. 7, A, B). Some earlier studies have investigated the effect of O_3 on forest carbon uptake. Cumulative stomatal uptake of 27 mmol m^{-2} over the growing season did not result in any visible damage or a reduction in NEE of a poplar plantation in Belgium (Zona et al., 2014). Zapletal (2011), on the other hand, reported that CO_2 uptake of a Norway spruce forest in the Czech Republic increased with increasing stomatal O_3 flux, followed by a sudden decrease in CO_2 uptake, suggesting that an O_3 flux threshold exists. Fares (2013) showed a negative correlation between GPP and O_3 uptake at two Mediterranean ecosystems (a forest dominated by *Pinus ponderosa* in California, USA and an orchard site of *Citrus sinensis* cultivated in California, USA). A GPP reduction of 1-16% in response to O_3 uptake under ambient O_3 concentrations of 30-50 ppb was determined across vegetation types and environmental conditions in the United States by Yue and Unger (2013). The magnitude of reduction depended on the sensitivity to O_3 of the species and on the biome types.

AOT40 is, at present, the European standard for forest protection (EEA, 2014), with a critical level of 5000 ppb h, equivalent to a growth reduction of 5 % (Mills et al., 2011). In this study on Scots pine in Brasschaat, this value was far exceeded in all years (Fig. 7), yet no negative effect on GPP was observed in years with higher AOT40 values. Particularly noteworthy is the extreme high AOT40-value of 2006, which was due to the high O_3 concentrations during that year, which, nevertheless, did not result in GPP reductions (Table 3).

POD_y is considered a more appropriate index for potential O_3 damage because it considers O_3 flux. The critical level of POD_1 is species-specific; a critical level of 8 mmol m^{-2} with 2 % growth reduction is used for Norway spruce and a critical level of 4 mmol m^{-2} with 4 % growth reduction is used for birch and beech (Mills et al., 2011). A critical level for Scots pine has not yet been determined and therefore the value of 8 mmol m^{-2} for Norway

Biogeosciences Discuss., doi:10.5194/bg-2016-12, 2016
Manuscript under review for journal Biogeosciences
Published: 23 February 2016

spruce is often adopted as critical level for Scots pine. During this study, this critical level was exceeded every single year, and again no negative correlation between total GPP residuals and POD_1 was observed. In comparison to the AOT40 level, 2006 was not the year with the highest POD_1. This difference between AOT40 and POD_1 during 2006 was due to stomatal closure; during high O_3 concentration events, g_{st} was rather low (Fig. 6). POD_1 was highest in the year 2002, when O_3 concentrations were relatively low, but g_{st} was high. The low O_3 concentrations explain the lower AOT40 for 2002.

Notwithstanding the absence of a statistically significant negative correlation between GPP residuals and both AOT40 and POD_y, critical levels for both AOT40 and POD_y were exceeded every single year. AOT40 is based on O_3 concentration and these concentration-based indices have been shown to be weaker indicators for O_3 damage than flux-based indices (Karlsson et al., 2007;Simpson et al., 2007). The critical level of POD_y for Scots pine was adopted from the critical level for Norway spruce (Mills et al., 2011). Possibly this critical level is too low for Scots pine. As shown by Reich (1987), pines are less sensitive to O_3 compared to hardwoods and crops. This supports the idea of a too low critical level.

Overall, no significant O_3 effects on GPP accumulated over the growing season were found. Although no significant O_3 effects on GPP were found in this study, it is still possible that O_3 negatively affected this Scots pine stand in Brasschaat. Stomatal O_3 uptake was linked to reductions in GPP only. As already stated in the introduction, protective responses such as compensation and enhanced tolerance occur in trees (Skärby et al., 1998). It is likely that trees at our study site were able to fully detoxify the incorporated O_3. As a result, no O_3 effects on carbon uptake were detectable. However, this protection may have come at a respiratory cost, which may have reduced the NPP/GPP ratio of this forest. The NPP/GPP ratio of our study site was very low (Gielen et al., 2013). In addition to the poor nutrient status (limitation by P and Mg, extremely high N deposition; (Neirynck et al., 2008)), O_3 uptake may partly be responsible. This can, however, not be tested because pine forest NPP data were not available at annual timescale.

5 Summary

We parameterised a multiplicative stomatal model for a Scots pine stand in Brasschaat. This species- and site-specific parameterised model performed very well. With this model, stomatal O_3 fluxes were calculated and used to test for O_3 effects on GPP. Only very small reductions in growing season GPP were calculated. Although critical levels for AOT40 and POD_y were exceeded in every single year, no significant negative correlations between total GPP residuals and stomatal O_3 flux, AOT40, and POD_y were found. In general, we can thus conclude that no O_3 effects were detected on the carbon uptake by the Scots pine stand in Brasschaat.

Biogeosciences Discuss., doi:10.5194/bg-2016-12, 2016
Manuscript under review for journal Biogeosciences
Published: 23 February 2016

Appendix A The multiplicative stomatal model

In this work the multiplicative stomatal model described by Jarvis (1976) is modified specific for the Scots pine stand in Brasschaat. The basic model is explained below.

The multiplicative stomatal model is described by Jarvis (1976) and modified by Emberson (2000);

$$g_{st} = g_{max} * f_{phen} * \max(f_{min}; f_{PAR} * f_T * f_{VPD} * f_{SWP}) \quad \text{(A1)}$$

where g_{max} is the species-specific maximum stomatal conductance to O_3 (mmol m^{-2} s^{-1}) expressed on a total leaf surface area basis. The other parameters are expressed in relative terms as a proportion of g_{max};

f_{min} is the ratio of g_{min} to g_{max}; where g_{min} is the minimal stomatal conductance that occurs during daylight period;

f_{phen} represents the modification of g_{max} due to phenological changes;

f_{PAR} represents the modification of g_{max} by photosynthetically active radiation (PAR);

f_T represents the modification of g_{max} by air temperature (T_{air});

f_{VPD} represents the modification of g_{max} by vapour pressure deficit (VPD);

f_{SWP} represents the modification of g_{max} by soil water potential (SWP).

Phenology modifies g_{max} because of the variation in g_{st} due to differences in needle age. The function can be modelled as follows:

(A2)

if $SGS \leq doy \leq (SGS + c)$, then $f_{PHEN} = f_{min} + (1 - f_{min}) * (1 - b) * \left(\frac{doy - SGS}{c}\right) + b$

if $SGS + c \leq doy \leq EGS - d$, then $f_{PHEN} = f_{min} + (1 - f_{min}) * 1$

if $EGS - d \leq doy \leq EGS$, then $f_{PHEN} = f_{min} + (1 - f_{min}) * (1 - b) * \left(\frac{EGS - doy}{d}\right) + b$

where SGS is the start of the growing season;

EGS is the end of the growing season;

Biogeosciences Discuss., doi:10.5194/bg-2016-12, 2016
Manuscript under review for journal Biogeosciences
Published: 23 February 2016

b, c, and d are species-specific parameters representing the minimum of f_{PHEN}, the number of days for f_{PHEN} to reach its maximum and the number of days during the decline of f_{PHEN} for the minimum to reach again, assuming linear increase and decrease at the start and end of the growing season.

The stomatal response PAR is described by a rectangular hyperbola, where a_{PAR} is a species-specific parameter determining the shape of the hyperbola (Emberson et al., 2000);

$$f_{PAR} = 1 - \exp(-a_{PAR} * PAR) \quad \text{(A3)}$$

The stomatal response to T_{air} is given by a parabolic function, where T_{min} is the minimum temperature at which stomatal opening occurs, and T_{opt} is the optimum temperature of stomatal opening (Emberson et al., 2000);

$$f_T = \max(0; 1 - \frac{(T - T_{opt})^2}{(T_{opt} - T_{min})^2}) \quad \text{(A4)}$$

The stomatal response to VPD is described by the following relationship, where VPD_{min} is a threshold for minimal stomatal opening, and VPD_{max} is a threshold for full stomatal opening (Emberson et al., 2000);

$$f_{VPD} = \min(1; \max\left(0; \frac{VPD_{min} - VPD}{VPD_{min} - VPD_{max}}\right)) \quad \text{(A5)}$$

The stomatal response to SWP is described by the following relationship, where SWP_{min} is a threshold for minimal stomatal opening, and SWP_{max} is a threshold for full stomatal opening (Emberson et al., 2000);

$$f_{SWP} = \min(1; \max\left(0; \frac{SWP_{min} - SWP}{SWP_{min} - SWP_{max}}\right)) \quad \text{(A6)}$$

Biogeosciences Discuss., doi:10.5194/bg-2016-12, 2016
Manuscript under review for journal Biogeosciences
Published: 23 February 2016

Appendix B Statistics of model performance

In order to test how well the modified stomatal model performed, several model statistics were calculated. These model statistics are explained below.

The mean bias (MB) is the mean difference between the simulations (S_i) and the observations (O_i), with n being the number of data points (Stone, 1993);

$$MB = n^{-1}\sum_{i=1}^{n}(S_i - O_i) \quad \text{(B1)}$$

The mean relative error (MRE) is the mean relative difference between the simulations and the observations (Peierls, 1935);

$$MRE = n^{-1}\sum_{i=1}^{n}\frac{|S_i - O_i|}{O_i} \quad \text{(B2)}$$

Willmott's index of agreement (d) is a dimensionless goodness-of-fit coefficient, with $\bar{O}$ being the mean observation (Willmott, 1981); The index can vary between 0 and 1, with d equals 1 for a perfect agreement between simulations and observations.

$$d = 1 - \frac{\sum_{i=1}^{n}(S_i - O_i)^2}{\sum_{i=1}^{n}(|S_i - \bar{O}| + |O_i - \bar{O}|)} \quad \text{(B3)}$$

The model efficiency (ME) gives an indication of how well the observations match the simulations (Nash & Sutcliffe, 1970); Model efficiency can range from -∞ to 1 and is 1 when simulations and observations match perfectly. An efficiency of 0 indicates that the simulations are as accurate as the mean observation and an efficiency of less than zero indicates that the mean observation is a better predictor than the model.

$$ME = 1 - \frac{\sum_{i=1}^{n}(S_i - O_i)^2}{\sum_{i=1}^{n}(O_i - \bar{O})^2} \quad \text{(B4)}$$

The root-mean-squared error (RMSE) is a measure of the mean absolute difference between the simulations and the observations, weighting large differences heavily (Willmott et al., 1985); The systematic component ($RMSE_s$) estimates the model's linear or systematic error, hence, the better the regression between simulations and observations, the smaller the systematic component (Willmott et al., 1985). The unsystematic component is a measure of how much of the discrepancy between simulations and observations is due to random processes (Willmott et al., 1985). A good model will provide low values of RMSE, with $RMSE_s$ close to zero and $RMSE_u$ close to RMSE (Willmott et al., 1985).

$$RMSE = \sqrt{n^{-1}\sum_{i=1}^{n}(S_i - O_i)^2} \quad \text{(B5)}$$

Biogeosciences Discuss., doi:10.5194/bg-2016-12, 2016
Manuscript under review for journal Biogeosciences
Published: 23 February 2016

$$RMSE_s = \sqrt{n^{-1}\sum_{i=1}^{n}(S'_i - O_i)^2} \quad \text{(B6)}$$

$$RMSE_u = \sqrt{n^{-1}\sum_{i=1}^{n}(S_i - S'_i)^2} \quad \text{(B7)}$$

$S'_i = a * O_i + b$, where 'a' and 'b' are slope and intercept, respectively, of the linear regression of the simulations versus the observations.

445

Biogeosciences Discuss., doi:10.5194/bg-2016-12, 2016
Manuscript under review for journal Biogeosciences
Published: 23 February 2016

Appendix C The canopy model

Stomatal conductance was calculated on leaf level with the stomatal model. The canopy model was used to scale up these values for the whole canopy. Ozone fluxes were calculated, based on an electrical conductance analogy. Below the general canopy model, including conductance analogy model, is explained, followed by the explanation of two submodel that were used: solar elevation submodel and radiation submodel.

Part 1 The canopy model

The canopy model is an algorithm to scale up g_{st} at leaf level to g_{st} at canopy level. Subsequently, O_3 fluxes are calculated with an electrical conductance analogy model, which calculates the instant canopy O_3 uptake from different input data Rg, T_{air}, VPD, LAI, SWP, and O_3 concentration. The canopy model consists of three submodels: the multiplicative stomatal model (Appendix A), the solar elevation submodel, and the radiation transfer submodel (see below).

First, the canopy is divided into different horizontal layers, with each a sunlit and shaded fraction. For each layer fraction the incoming PAR is calculated with the radiation transfer submodel. With the multiplicative stomatal model g_{st} is calculated for each layer fraction.

For each layer fraction the total leaf conductance (mol m^{-2} leaf area s^{-1}) is calculated by summing g_{st} and g_{ns}, the non-stomatal conductance. This value is multiplied by LAI of the layer fraction and the values for both the sunlit and the shaded layer fraction are summed to obtain the total layer conductance (mol m^{-2} ground area s^{-1}). All layer conductances can be summed to obtain the conductance of the canopy as a whole (g_{can}).

The total conductance is a function of g_{bl} and g_{can} based on an electrical conductance analogy model.

$$g_{tot} = \left(\frac{1}{g_{aero}} + \frac{1}{g_{bl}} + \frac{1}{g_{can}}\right)^{-1} \quad \text{(C1)}$$

where g_{aero} is the aerodynamic conductance; g_{bl} is the boundary layer conductance; g_{can} is the canopy conductance.

Total O_3 flux (nmol m^{-2} ground area s^{-1}) is the O_3 flux for the whole canopy and is then calculated by:

$$F_{tot} = [O_3] * g_{tot} \quad \text{(C2)}$$

where $[O_3]$ is the O_3 concentration (ppb).

Stomatal O_3 flux is the fraction of the total O_3 flux taken up by the stomata and is calculated by:

Biogeosciences Discuss., doi:10.5194/bg-2016-12, 2016
Manuscript under review for journal Biogeosciences
Published: 23 February 2016

$$F_{st} = [O_3] * \frac{g_{st}}{g_{st}+g_{ns}} \quad \text{(C3)}$$

where g_{st} is the stomatal conductance (mol m^{-2} ground area s^{-1}); g_{ns} is the non-stomatal conductance (mol m^{-2} ground area s^{-1}).

Non-stomatal O_3 flux (F_{ns}) is the difference between total O_3 flux and stomatal O_3 flux:

$$F_{ns} = F_{tot} - F_{st} \quad \text{(C4)}$$

Part 2 The solar elevation submodel

This submodel calculates the solar elevation angle, β (radians), at each time step (Campbell and Norman, 1998).

$$\beta = \arcsin(\sin\phi \sin\delta + \cos\phi \cos\delta \cos h) \quad \text{(C5)}$$

where δ is the solar declination angle; $\delta = -23.4 * \left(\frac{\pi}{180}\right) * \cos(2 * \pi * \frac{doy+10}{365})$

ϕ is the latitude in radians; $\phi = 0.89$

h is the hour angle of the sun; $h = \pi * \frac{t-t_0}{12.0}$

where t is time; t_0 is solar noon; $t_0 = 12 + \frac{4*(L_s-L_e)-E_t}{60.0}$

L_s is the standard longitude in degrees; $L_s = 15.0$

L_i is the local longitude in degrees; $L_i = 4.0$

E_t is the empheris of the sun;

$$E_t = 0.017 + 0.4281 * \cos(F_d) - 7.351 * \sin(F_d) - 3.349 * \cos(2 * F_d) - 9.731 * \sin(F_d)$$

where F_d is the day angle; $F_d = 2 * \pi * \frac{doy-1}{365}$

Part 3 The radiation transfer submodel

The radiation submodel calculates the direct (I_{b0}) and diffuse (I_{d0}) fraction of the incoming radiation (I) at the top of the canopy. Hence, I is equal to R_g. These calculation is based on the difference between

Biogeosciences Discuss., doi:10.5194/bg-2016-12, 2016
Manuscript under review for journal Biogeosciences
Published: 23 February 2016

measured and theoretically potential incoming radiation above the canopy, which is depending on β, the solar elevation angle (Op de Beeck et al., 2010).

First the sunlit LAI fraction of each horizontal leaf layer i is calculated with Beer's law:

$$f_{sun(i)} = \exp(-k_b \Omega LAI_{c(i)}) \quad \text{(C6)}$$

where k_b is the direct radiation extinction coefficient; Ω is a factor accounting for inter- and intra-crown foliage clumping; $LAI_{c(i)}$ is the cumulative LAI above a horizontal leaf layer i.

A spherical needle angle distribution is assumed, hence $k_b = 0.5/\sin\beta$ (de Pury, 1997).

The shaded LAI fraction of each horizontal leaf layer i is calculated as follows:

$$f_{shad(i)} = 1 - f_{sun(i)} \quad \text{(C7)}$$

where fsun(i) is the sunlit LAI fraction.

The intensity of direct radiation does not decline through the canopy, but the diffuse radiation does and is calculated with Beer's law:

$$I_{d(i)} = I_{d0} * \exp(k_d \Omega LAI_{c(i)}) \quad \text{(C8)}$$

where I_{d0} is the incoming diffuse radiation.

The total received radiation by a sunlit fraction ($I_{sun(i)}$) is the sum of direct and diffuse radiation. Shaded leaves only receive diffuse radiation:

$$I_{shad(i)} = I_{d(i)} \quad \text{(C9)}$$

$$I_{sun(i)} = \cos\left(\frac{\pi}{3}\right) * I_{b0} + I_{d(i)} \quad \text{(C10)}$$

where $\left(\frac{\pi}{3}\right)$ is the averaged leaf angle for a uniform needle angle distribution; I_{b0} is the incoming direct radiation at top of the canopy; $I_{d(i)}$ is the diffuse radiation for a horizontal leaf layer i.

Total received irradiance is now converted to total received PAR and split into PAR per horizontal leaf layer.

Author contribution L Verryckt, M. Op de Beeck, B. Gielen, M. Roland and I.A. Janssens designed the study. J. Neirynck provided the O_3 concentration measurements, B. Gielen provided the EC and LAI data, B. Gielen, M. Op de Beeck and L. Verryckt measured g_{st} in sity, and M. Op de Beeck and L. Verryckt conducted the modelling. All authors contributed to the writing.

Acknowledgement The measurements for this work were funded by the Hercules Foundation, through support of the Brasschaat ICOS ecosystem station. IAJ acknowledges support from the European Research Council Synergy grant ERC-2013-SyG-610028 IMBALANCE-P.

References

Andersen, C. P., Wilson, R., Plocher, M., and Hogsett, W. E.: Carry-over effects of ozone on root growth and carbohydrate concentrations of ponderosa pine seedlings, Tree Physiol, 17, 805-811, 1997.

Baldocchi, D. D., Hicks, B. B., and Camara, P.: A canopy stomatal resistance model for gaseous deposition to vegetated surfaces, Atmos Environ, 21, 91-101, http://dx.doi.org/10.1016/0004-6981(87)90274-5, 1987.

Beedlow, P. A., Tingey, D. T., Phillips, D. L., Hogsett, W. E., and Olszyk, D. M.: Rising atmospheric CO_2 and carbon sequestration in forests, Front Ecol Environ, 2, 315-322, 2004.

Buker, P., Feng, Z., Uddling, J., Briolat, A., Alonso, R., Braun, S., Elvira, S., Gerosa, G., Karlsson, P. E., Le Thiec, D., Marzuoli, R., Mills, G., Oksanen, E., Wieser, G., Wilkinson, M., and Emberson, L. D.: New flux based dose-response relationships for ozone for European forest tree species, Environ Pollut, 206, 163-174, 10.1016/j.envpol.2015.06.033, 2015.

Campbell, G. S., and Norman, J. M.: Radiation fluxes in natural environments, in: An introduction to environmental biophysics, Springer, New York, 167-184, 1998b.

Carrara, A., Kowalski, A. S., Neirynck, J., Janssens, I. A., Yuste, J. C., and Ceulemans, R.: Net ecosystem CO2 exchange of mixed forest in Belgium over 5 years, Agr Forest Meteorol, 119, 209-227, 10.1016/s0168-1923(03)00120-5, 2003.

Carrara, A., Janssens, I. A., Curiel Yuste, J., and Ceulemans, R.: Seasonal changes in photosynthesis, respiration and NEE of a mixed temperate forest, Agr Forest Meteorol, 126, 15-31, 10.1016/j.agrformet.2004.05.002, 2004.

Chappelka, A. H., and Samuelson, L. J.: Ambient ozone effects on forest trees of eastern United States: a review, New Phytol, 139, 91-108, 1998.

Cieslik, S. A.: Ozone uptake by various surface types: a comparison between dose and exposure, Atmos Environ, 38, 2409-2420, 10.1016/j.atmosenv.2003.10.063, 2004.

CLRTAP: Mapping Critical Levels for Vegetation, Chapter III of Manual on methodologies and criteria for modelling and mapping critical loads and levels and air pollution effects, risks and trends., UNECE Convention on Long-range Transboundary Air Pollution, 2015, http://www.icpmapping.org, access: December 2015.

Darall, N. M.: The effect of air pollutants on physiological processes in plants, Plant Cell Environ, 12, 1-30, 1989.

de Pury, D. G. G. F., G. D.: Simple scaling of photosynthesis from leaves to canopies without the errors of big-leaf models, Plant Cell Environ, 20, 537-557, 1997.

European Environment Agency: http://www.eea.europa.eu/, access: 1 May, 2014.

Emberson, L. D., Ashmore, M. R., Cambridge, H. M., Simpson, D., and Tuovinen, J. P.: Modelling stomatal ozone flux across Europe, Environ Pollut, 109, 403-413, 2000.

Falge, E., Baldocchi, D., Olson, R., Anthoni, P., Aubinet, M., Bernhofer, C., Burba, G., Ceulemans, R., Clement, R., Dolman, H., Granier, A., Gross, P., Grünwald, T., Hollinger, D., Jensen, N.-O., Katul, G., Keronen, P., Kowalski, A., Ta Lai, C., Law, B. E., Meyers, T., Moncrieff, J., Moors, E., Munger, J. W., Pilegaard, K., Rannick, Ü., Rebmann, C., Suyker, A., Tenhunen, J., Tu, K., Verma, S., Vesala, T., Wilson, K., and Wofsy, S.: Gap filling strategies for long term energy flux data sets, Agr Forest Meteorol, 107, 71-77, 2001.

Fares, S., McKay, M., Holzinger, R., and Goldstein, A. H.: Ozone fluxes in a Pinus ponderosa ecosystem are dominated by non-stomatal processes: Evidence from long-term continuous measurements, Agr Forest Meteorol, 150, 420-431, http://dx.doi.org/10.1016/j.agrformet.2010.01.007, 2010.

Fares, S., Vargas, R., Detto, M., Goldstein, A. H., Karlik, J., Paoletti, E., and Vitale, M.: Tropospheric ozone reduces carbon assimilation in trees: estimates from analysis of continuous flux measurements, Glob Chang Biol, 19, 2427-2443, 10.1111/gcb.12222, 2013.

Gerosa, G., Vitale, M., Finco, A., Manes, F., Denti, A., and Cieslik, S.: Ozone uptake by an evergreen Mediterranean Forest in Italy. Part I: Micrometeorological flux measurements and flux partitioning, Atmos Environ, 39, 3255-3266, 10.1016/j.atmosenv.2005.01.056, 2005.

Gielen, B., Verbeeck, H., Neirynck, J., Sampson, D. A., Vermeiren, F., and Janssens, I. A.: Decadal water balance of a temperate Scots pine forest (*Pinus sylvestris* L.) based on measurements and modelling, Biogeosciences, 7, 1247-1261, 2010.

Gielen, B., Neirynck, J., Luyssaert, S., and Janssens, I. A.: The importance of dissolved organic carbon fluxes for the carbon balance of a temperate Scots pine forest, Agr Forest Meteorol, 151, 270-278, 10.1016/j.agrformet.2010.10.012, 2011.

Gielen, B., De Vos, B., Campioli, M., Neirynck, J., Papale, D., Verstraeten, A., Ceulemans, R., and Janssens, I. A.: Biometric and eddy covariance-based assessment of decadal carbon sequestration of a temperate Scots pine forest, Agr Forest Meteorol, 174-175, 135-143, 10.1016/j.agrformet.2013.02.008, 2013.

Gond, V., De Pury, D. G. G., Veroustraete, F., and Ceulemans, R.: Seasonal variations in leaf area index, leaf chlorophyll, and water content; scaling-up to estimate fAPAR and carbon balance in a multilayer, multispecies temperate forest, Tree Physiol., 19, 673-679, 1999.

Goudriaan, J.: Crop micrometeorology: a Simulation Study, Pudoc, edited by: Documentation, C. f. A. P. a., Wageningen, The Netherlands, 249, 1977.

Grüters, U., Fangmeier, A., and Jäger, H.-J.: Modelling stomatal responses of spring wheat (*Triticum aestivum* L. cv. Turbo) to ozone and different levels of water supply, Environ Pollut, 87, 141-149, 1995.

ICP Vegetation: Ozone pollution: impacts on carbon sequestration in Europe, Eds Harmens H. and Mills G., Bangor, UK, NERC/Centre for Ecology & Hydrology, 1-90, 2012.

IPCC: Climate Change 2007: Synthesis Report. Contribution of Working groups I, II and III to the Fourth Assessment Report of the Intergovernmental Panel on Climate Change [Core Writing Team, Pachauri, R.K. and Reisinger, A. (eds.)], IPCC, Geneva, Switzerland, 104, 2007.

Janssens, I. A., Sampson, D. A., Cermak, J., Meiresonne, L., Riguzzi, F., Overloop, S., and Ceulemans, R.: Above- and belowground phytomass and carbon storage in a Belgian Scots pine stand, Ann. For. Sci. 56, 81-90, 1999.

Jarvis, P. G.: The interpretation of the variations in leaf water potential and stomatal conductance found in canopies in the field, Philosophical Transactions of the Royal Society of Londen. Series B. Biological Sciences., 273, 593-610, 1976.

Jonckheere, I., Muys, B., and Coppin, P.: Allometry and evaluation of in situ optical LAI determination in Scots pine: a case study in Belgium, Tree Physiol., 25, 2005.

Karlsson, P. E., Uddling, J., Braun, S., Broadmeadow, M., Elvira, S., Gimeno, B. S., Le Thiec, D., Oksanen, E., Vandermeiren, K., Wilkinson, M., and Emberson, L.: New critical levels for ozone effects on young trees based on AOT40 and simulated cumulative leaf uptake of ozone, Atmos Environ, 38, 2283-2294, 10.1016/j.atmosenv.2004.01.027, 2004.

Karlsson, P. E., Braun, S., Broadmeadow, M., Elvira, S., Emberson, L., Gimeno, B. S., Le Thiec, D., Novak, K., Oksanen, E., Schaub, M., Uddling, J., and Wilkinson, M.: Risk assessments for forest trees: the performance of the ozone flux versus the AOT concepts, Environ Pollut, 146, 608-616, 10.1016/j.envpol.2006.06.012, 2007.

Konôpka, B., Yuste, J. C., Janssens, I. A., and Ceulemans, R.: Comparison of Fine Root Dynamics in Scots Pine and Pedunculate Oak in Sandy Soil, Plant Soil, 276, 33-45, 10.1007/s11104-004-2976-3, 2005.

Martin, T. A., Brown, K. J., Carmák, J., Ceulemans, R., Kucera, J., Meinzer, F. C., Rombold, J. S., Sprugel, D. G., and Hinckley, T. M.: Crown conductance and tree and stand transpiration in a second growth Abies amibilis forest, Can. J. For. Res., 27, 797-808, 1997.

Mauzerall, D. L., and Wang, X.: Protecting agricultural crops from the effects of tropospheric ozone exposure: Reconciling Science and Standard Setting in the United States, Europe, and Asia, Annu Rev Energ Env, 26, 237-268, doi:10.1146/annurev.energy.26.1.237, 2001.

McLaughlin, S. B., Nosal, M., Wullschleger, S. D., and Sun, G.: Interactive effects of ozone and climate on tree growth and water use in a southern Appalachian forest in the USA, New Phytol, 174, 109-124, 10.1111/j.1469-8137.2007.02018.x, 2007.

Middleton, J. T.: Response of Plants to Air Pollution, Journal of the Air Pollution Control Association, 6, 7-9, 10.1080/00966665.1956.10467730, 1956.

Mikkelsen, T. N., Ro-Poulsen, H., Hovmand, M. F., Jensen, N. O., Pilegaard, K., and Egeløv, A. H.: Five-year measurements of ozone fluxes to a Danish Norway spruce canopy, Atmos Environ, 38, 2361-2371, http://dx.doi.org/10.1016/j.atmosenv.2003.12.036, 2004.

Mills, G., Pleijel, H., Büker, P., Braun, S., Emberson, L., Harmens, H., Hayes, F., Simpson, D., Grünhage, L., Karlsson, P.-E., Danielsson, H., Bermejo, V., and Fernández, I. G.: Mapping critical levels for vegetation, in: Manual on methodologies and criteria for Modelling and Mapping Critical Loads & Levels and Air Pollution Effects, Risks and Trends, III.1-III.114, 2011.

Musselman, R. C., and Massman, W. J.: Ozone flux to vegetation and its relationship to plant response and ambient air quality standards, Atmos Environ, 33, 65-73, 1999.

Neirynck, J., Janssens, I. A., Roskams, P., Quataert, P., Verschelde, P., and Ceulemans, R.: Nitrogen biogeochemistry of a mature Scots pine forest subjected to high nitrogen loads, Biogeochemistry, 91, 201-222, 10.1007/s10533-008-9280-x, 2008.

Neirynck, J., Gielen, B., Janssens, I. A., and Ceulemans, R.: Insights into ozone deposition patterns from decade-long ozone flux measurements over a mixed temperate forest, J Environ Monit, 14, 1684-1695, 10.1039/c2em10937a, 2012.

Noble, R. D., and Jensen, K. F.: Effects of sulfur dioxide and ozone on growth of hybrid poplar leaves, Am J Bot, 67, 1005-1009, 1980.

Op de Beeck, M., Gielen, B., Jonckheere, I., Samson, R., Janssens, I. A., and Ceulemans, R.: Needle age-related and seasonal photosynthetic capacity variation is negligible for modelling yearly gas exchange of a sparse temperate Scots pine forest, Biogeosciences, 7, 199-215, 2010.

Paoletti, E., and Grulke, N. E.: Ozone exposure and stomatal sluggishness in different plant physiognomic classes, Environ Pollut, 158, 2664-2671, 10.1016/j.envpol.2010.04.024, 2010.

Peierls, R.: Statistical Error in Counting Experiments, Proc R Soc Lond A, 149, 467-486, 10.1098/rspa.1935.0076, 1935.

Reich, P. B., and Amundson, R. G.: Ambient levels of ozone reduce net photosynthesis in tree and crop species, Science, 230, 566-570, 1985.

Reich, P. B.: Quantifying plant response to ozone - a unifying theory, Tree Physiol, 3, 63-91, 1987.

Samuelson, L. J.: Ozone-exposure responses of black-cherry and red maple seedlings, Environ Exp Bot, 34, 355-362, 10.1016/0098-8472(94)90017-5, 1994.

Simpson, D., Ashmore, M. R., Emberson, L., and Tuovinen, J. P.: A comparison of two different approaches for mapping potential ozone damage to vegetation. A model study, Environ Pollut, 146, 715-725, 10.1016/j.envpol.2006.04.013, 2007.

Skärby, L., Troeng, E., and Boström, C. A.: Ozone uptake and effects on transpiration, net photosynthesis and dark respiration in Scots pine, For. Sci., 33, 801-808, 1987.

Skärby, L., Ro-Poulsen, H., Wellburn, F. A. M., and Sheppard, L. J.: Impacts of ozone on forests: a European perspective, New Phytol, 139, 109-122, 1998.

Stone, R. J.: Improved statistical procedure for the evaluation of solar radiation estimation models, Sol Energy, 51, 289-291, 1993.

van Genuchten, M. T.: A Closed-form Equation for Predicting the Hydraulic Conductivity of Unsaturated Soils, Soil Sci Soc Am J, 44, 892-898, 10.2136/sssaj1980.03615995004400050002x, 1980.

Vitale, M., Gerosa, G., Ballarindenti, A., and Manes, F.: Ozone uptake by an evergreen mediterranean forest (L.) in Italy—Part II: flux modelling. Upscaling leaf to canopy ozone uptake by a process-based model, Atmos Environ, 39, 3267-3278, 10.1016/j.atmosenv.2005.01.057, 2005.

Willmott, C. J.: On the validation of models, Phys Geogr, 2, 184-194, 1981.

Willmott, C. J., Ackleson, S. G., Davis, R. E., Feddema, J. J., Klink, K. M., Legates, D. R., O'Donnell, J., and Rowe, C. M.: Statistics for the evaluation and comparison of models, J Geophys Res, 90, 8995-9005, 1985.

Yue, X., and Unger, N.: Ozone vegetation damage effects on gross primary productivity in the United States, Atmos Chem Phys Discussions, 13, 31563-31605, 10.5194/acpd-13-31563-2013, 2013.

Yuste, J. C., Konôpka, B., Janssens, I. A., Coenen, K., Xiao, C. W., and Ceulemans, R.: Contrasting net primary productivity and carbon distribution between neighboring stands of Quercus robur and Pinus sylvestris, Tree Physiol., 25, 701-712, 2005.

Zapletal, M., Cudlin, P., Chroust, P., Urban, O., Pokorny, R., Edwards-Jonasova, M., Czerny, R., Janous, D., Taufarova, K., Vecera, Z., Mikuska, P., and Paoletti, E.: Ozone flux over a Norway spruce forest and correlation with net ecosystem production, Environ Pollut, 159, 1024-1034, 10.1016/j.envpol.2010.11.037, 2011.

Zona, D., Gioli, B., Fares, S., De Groote, T., Pilegaard, K., Ibrom, A., and Ceulemans, R.: Environmental controls on ozone fluxes in a poplar plantation in Western Europe, Environ Pollut, 184, 201-210, 2014.

Biogeosciences Discuss., doi:10.5194/bg-2016-12, 2016
Manuscript under review for journal Biogeosciences
Published: 23 February 2016

675 Table 1. Optimised parameter values of the multiplicative stomatal model.

g_{min} (mol O_3 m^{-2} s^{-1})	0.02
g_{max} (mol O_3 m^{-2} s^{-1})	0.14
a	0.0057
T_{opt} (°C)	25.61
T_{min} (°C)	5.47
VPD_{min} (kPa)	3.16
VPD_{max} (kPa)	0.51
SWP_{min} (MPa)	-1.18
SWP_{max} (MPa)	-0.19

Biogeosciences Discuss., doi:10.5194/bg-2016-12, 2016
Manuscript under review for journal Biogeosciences
Published: 23 February 2016

Table 2. Statistics of the model evaluation. The statistics used to evaluate the model performance are mean bias (MB), relative mean error (RME), systematic and unsystematic root mean squared error ($RMSE_{s/u}$), Willmott's index of agreement (d), model efficiency (ME), coefficient of determination (R^2).

Statistics	**Parameterisation**	**Validation**
MB	0.002	0.002
RME	0.34	0.33
RMSE	0.019	0.019
$RMSE_s$	0.006	0.006
$RMSE_u$	0.017	0.017
d	0.99	0.99
ME	0.72	0.72
R^2	0.72	0.72

Biogeosciences Discuss., doi:10.5194/bg-2016-12, 2016
Manuscript under review for journal Biogeosciences
Published: 23 February 2016

Table 3. GPP values (mol C m^{-2} day^{-1}) for the days with low stomatal O_3 uptake, high stomatal O_3 uptake, and the growing season total (GS) of different years as well as the multi-annual mean. One GPP model (GPPmod1) was trained without days with high stomatal O_3 uptake, whereas a second GPP model (GPPmod2) also excluded days following high O_3 events, and was thus trained to test for lag effects of O_3. The relative difference between modelled and EC-derived GPP estimates is presented between brackets. Positive values indicate an overestimation by the model and therefore a potential O_3 effects on GPP.

	Days with low stomatal O_3 uptake			Days with high stomatal O_3 uptake			Growing Season Total		
Year	GPPmea	GPPmod1	GPPmod2	GPPmea	GPPmod1	GPPmod2	GPPmea	GPPmod1	GPPmod2
1998	0.47	0.43 (-7%)	0.38 (-20%)	0.76	0.56 (-2%)	0.57 (-26%)	0.48	0.44 (-9%)	0.39 (-22%)
2000	0.48	0.46 (-4%)	0.48 (+0%)	0.70	0.65 (-7%)	0.70 (-0%)	0.49	0.47 (-4%)	0.49 (+0%)
2001	0.43	0.42 (-1%)	0.37 (-13%)	0.64	0.51 (-20%)	0.45 (-29%)	0.44	0.43 (-3%)	0.38 (-14%)
2002	0.39	0.40 (+4%)	0.38 (-2%)	0.57	0.52 (-7%)	0.50 (-11%)	0.40	0.41 (+3%)	0.39 (-2%)
2004	0.42	0.40 (-3%)	0.41 (-2%)	0.56	0.55 (-3%)	0.59 (+4%)	0.43	0.41 (-3%)	0.42 (-2%)
2005	0.41	0.40 (-3%)	0.41 (-1%)	0.62	0.57 (-7%)	0.56 (-9%)	0.42	0.41 (-3%)	0.42 (-1%)
2006	0.45	0.41 (-10%)	0.37 (-19%	0.76	0.58 (-24%)	0.45 (-42%)	0.47	0.42 (-13%)	0.37 (-24%)
2007	0.44	0.45 (+2%)	0.45 (+3%)	0.76	0.64 (-17%)	0.64 (-17%)	0.46	0.46 (-2%)	0.46 (-1%)
2008	0.47	0.47 (-0.4%)	0.67 (+44%)	0.84	0.75 (-10%)	0.74 (-12%)	0.49	0.48 (-2%)	0.68 (+40%)
2009	0.51	0.49 (-4%)	0.64 (+24%)	0.80	0.78 (-3%)	0.76 (-6%)	0.57	0.51 (-12%)	0.64 (15%)
2010	0.47	0.53 (+13%)	0.57 (+21%)	0.74	0.74 (+0%)	0.76 (+3%)	0.49	0.54 (+10%)	0.58 (+16%)
2011	0.60	0.55 (-8%)	0.55 (-8%)	0.82	0.76 (-7%)	0.80 (-2%)	0.64	0.56 (-14%)	0.56 (-14%)
2012	0.64	0.62 (-3%)	0.63 (-2%)	1.06	0.92 (-13%)	1.01 (-5%)	0.66	0.64 (-4%)	0.64 (-3%)
2013	0.52	0.56 (+7%)	0.56 (+6%)	0.81	0.79 (-2%)	0.92 (+14%)	0.55	0.58 (+5%)	0.58 (+5%)
Mean	0.48	0.47	0.49	0.75	0.67	0.67	0.50	0.48	0.50

Biogeosciences Discuss., doi:10.5194/bg-2016-12, 2016
Manuscript under review for journal Biogeosciences
Published: 23 February 2016

Fig. 1. Fingerprint of the meteorological and eddy-flux derived gross primary productivity (GPP) measurements averaged over the period 1998-2013. Day of year is plotted on the y-axis and hour of day on the x-axis. Air temperature (T_{air}), incoming global radiation (Rg), vapour pressure deficit (VPD), and GPP are plotted.

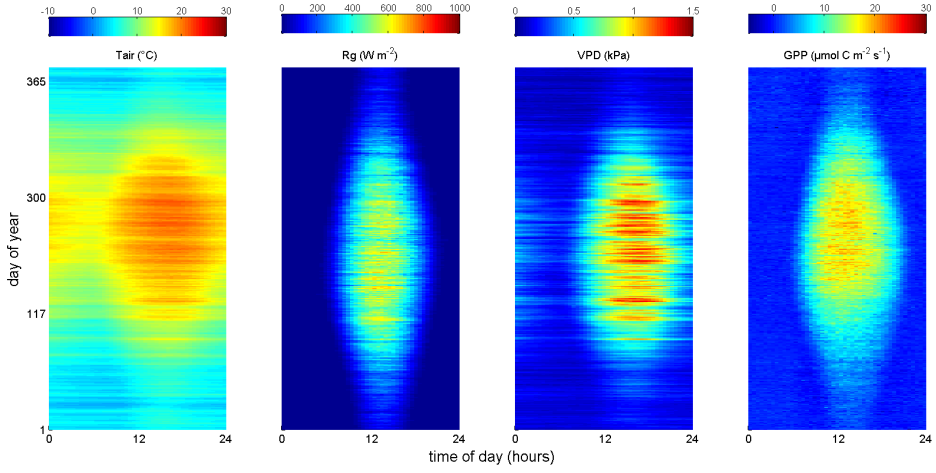

695

Biogeosciences Discuss., doi:10.5194/bg-2016-12, 2016
Manuscript under review for journal Biogeosciences
Published: 23 February 2016

Fig. 2.Time series of the weekly total precipitation and mean soil water potential (SWP). The precipitation and SWP data are averaged over the period 1998-2013. Error bars represent the 95% confidence intervals.

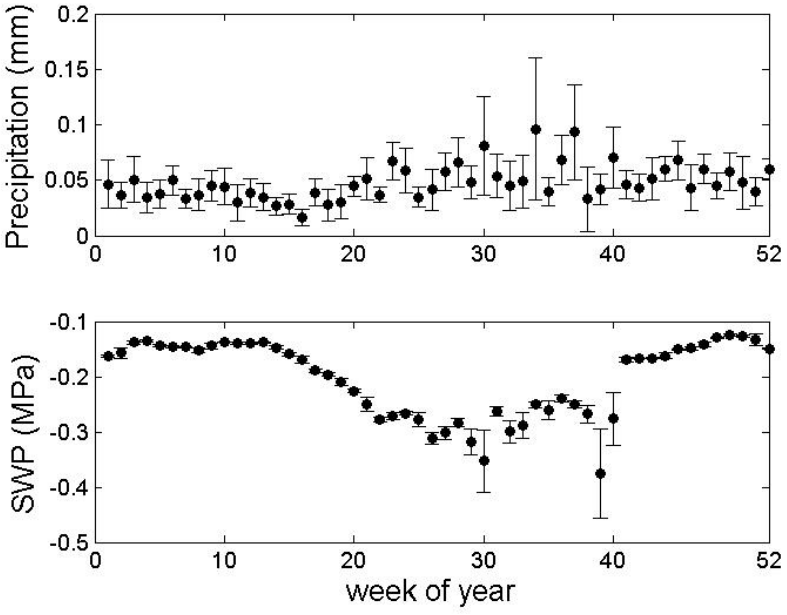

700

Biogeosciences Discuss., doi:10.5194/bg-2016-12, 2016
Manuscript under review for journal Biogeosciences
Published: 23 February 2016

Fig. 3. Seasonal changes of LAI over the 15 year study period at the Brasschaat Scots pine site.

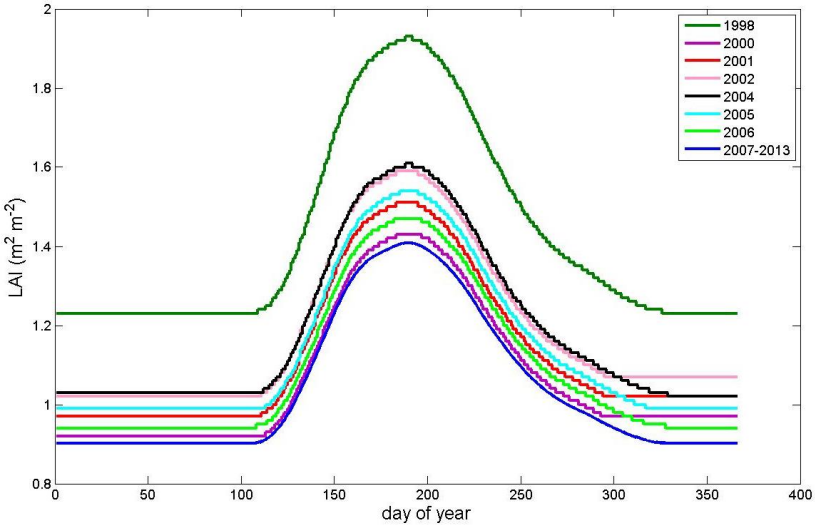

705

Biogeosciences Discuss., doi:10.5194/bg-2016-12, 2016
Manuscript under review for journal Biogeosciences
Published: 23 February 2016

Fig. 4. Measured versus modelled stomatal conductance (g_{st}) for parameterisation dataset (A) (n = 205) and validation dataset (B) (n = 205). The black line is the 1:1 line. The red line is the linear fit for which the equation is given in the figure. The p-values of the slope (p_a) and the intercept (p_b) are also shown.

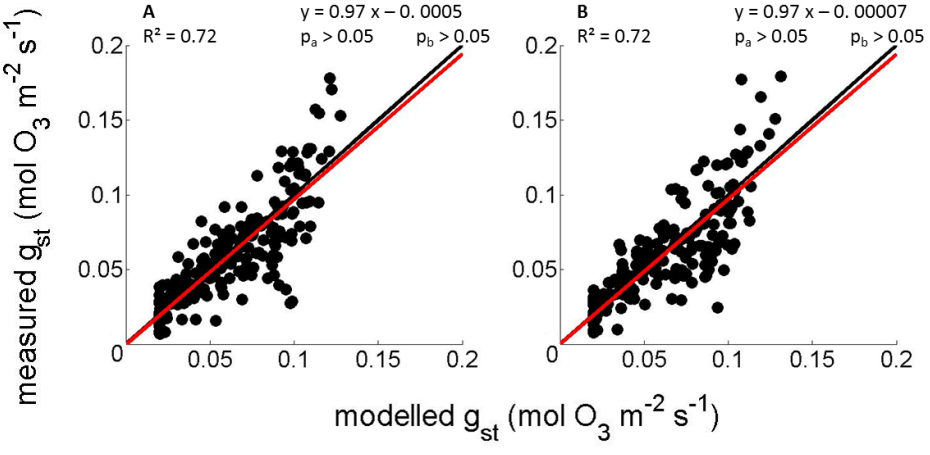

710

Biogeosciences Discuss., doi:10.5194/bg-2016-12, 2016
Manuscript under review for journal Biogeosciences
Published: 23 February 2016

Biogeosciences Discussions
Open Access
EGU

Fig. 5. Measured stomatal conductance (g_{st}) in function of the different variables used in the multiplicative model: photosynthetically active radiation (PAR), air temperature (T_{air}), vapour pressure deficit (VPD), and soil water potential (SWP). The red line represents the boundary line for which the functions are given in Appendix A (A3-A6). (n = 205)

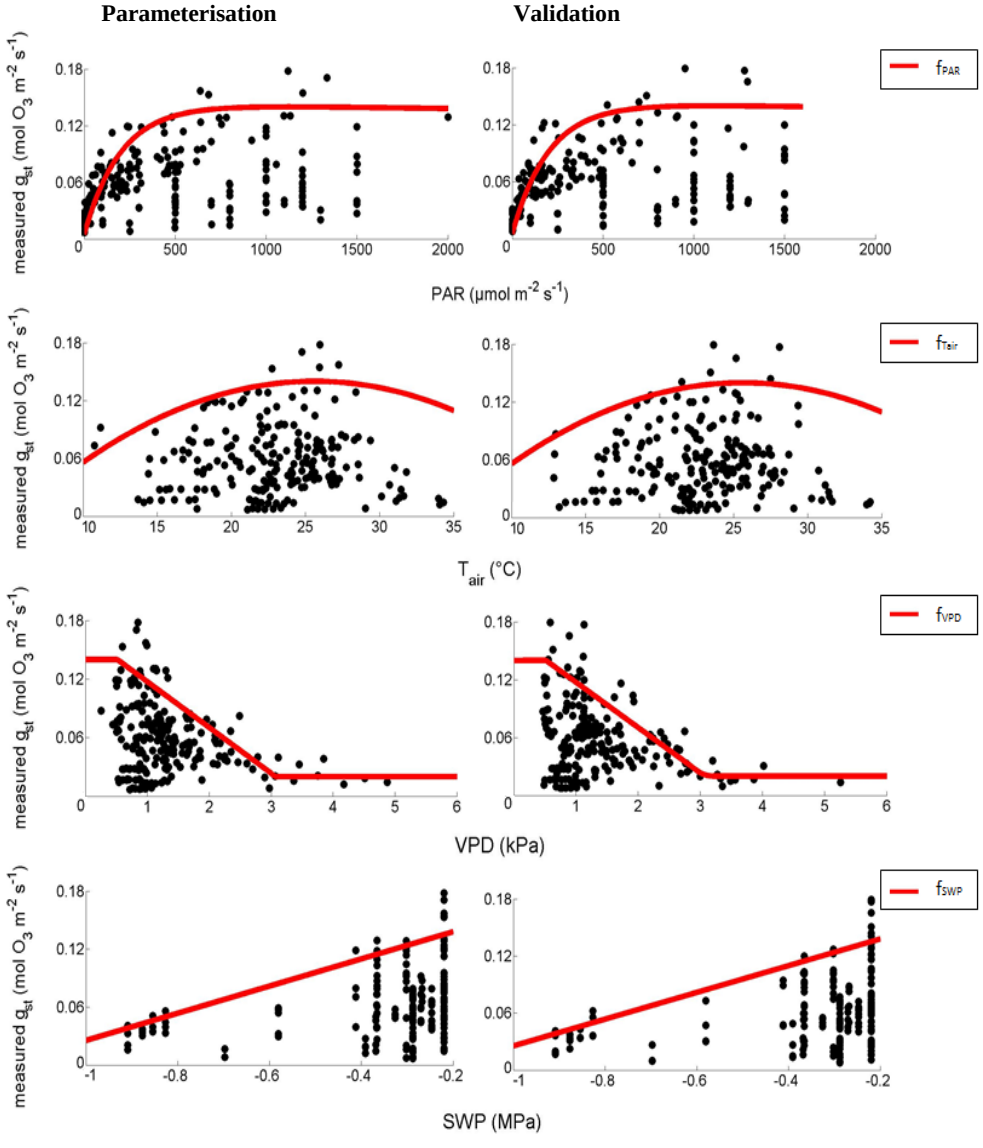

Biogeosciences Discuss., doi:10.5194/bg-2016-12, 2016
Manuscript under review for journal Biogeosciences
Published: 23 February 2016

Fig. 6. Fingerprints of stomatal conductance (g_{st}), ozone concentration ([O_3]), and stomatal (F_{st}), non-stomatal (F_{ns}), and total ozone flux (F_{tot}). Day of year is plotted on the y-axis and hour of day on the x-axis. Please note the different scales for F_{st}, F_{ns}, and F_{tot}.

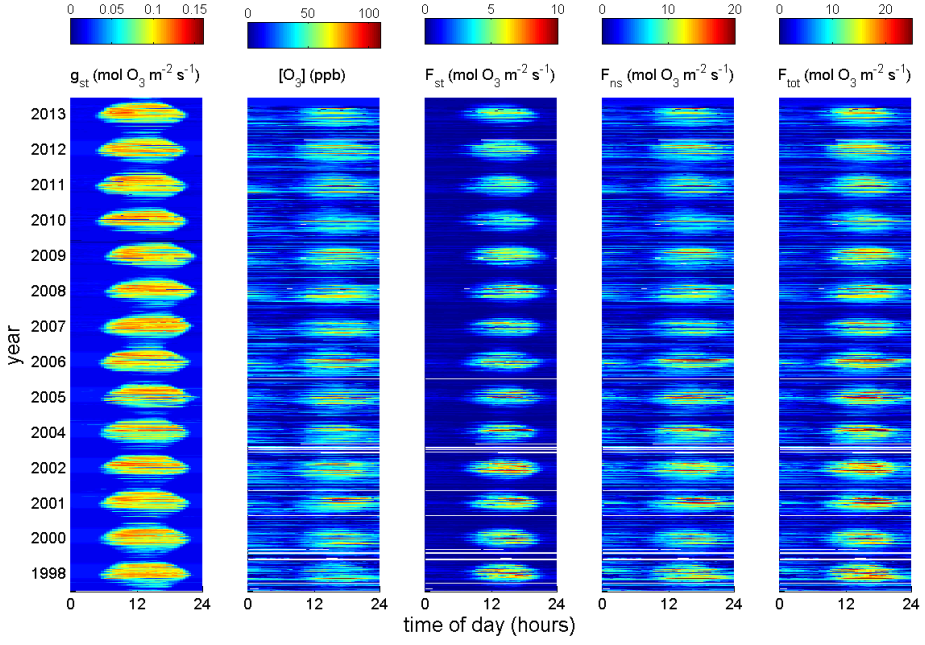

Biogeosciences Discuss., doi:10.5194/bg-2016-12, 2016
Manuscript under review for journal Biogeosciences
Published: 23 February 2016

Fig. 7. Gross primary productivity (GPP)-model residuals in function of total stomatal ozone flux over the growing season (F_{st}; panels A, B), AOT40 (panels C, D), POD_1 (panels E, F), and POD_2 (panels G, H). The GPP model of (A), (C), (E), and (G) was trained without days with high stomatal O_3 uptake, whereas the GPP model of (B), (D), (F), and (H) was trained to test for possible lag effects of O_3 on GPP. The vertical dashed lines represent the threshold values used in Europe (C – H). For each relation a linear function was fitted, but none were statistically significant as indicated in the panels (n = 14).

Biogeosciences Discuss., doi:10.5194/bg-2016-12, 2016
Manuscript under review for journal Biogeosciences
Published: 23 February 2016